The Eurasia Proceedings of Science, Technology, Engineering and Mathematics (EPSTEM)
ISSN: 2602-3199

The Eurasia Proceedings of Science, Technology, Engineering and Mathematics (EPSTEM), 2026

Volume 40, Pages 526-536

ICBAST 2026: International Conference on Basic Sciences and Technology

Physics-Informed Neural Networks (PINNs) for Parameter Estimation in the SIRS-D Epidemiological Model

Fitri Cahyani
Gadjah Mada University

Abdurakhman Abdurakhman
Gadjah Mada University

Chyntia Meininda Anjanni
Gadjah Mada University

Abstract: Infectious diseases exhibit complex and rapidly evolving transmission dynamics, requiring modeling approaches that can accurately capture these mechanisms. The SIRS-D compartmental model provides a suitable framework, as it incorporates temporary immunity and disease-induced mortality within the epidemic process. Accurate parameter estimation is essential for quantifying the transmission rate, recovery rate, waning immunity rate, and mortality rate, which collectively govern the system behavior. Among existing estimation methods, Physics-Informed Neural Networks (PINNs) offer significant advantages by integrating observational data with the underlying structure of differential equations, thereby preserving physical consistency while maintaining robustness under imperfect data conditions. In this study, PINNs are employed to estimate the parameters of the SIRS-D model using synthetic data generated through the fourth-order Runge–Kutta (RK4) method to ensure stable and consistent numerical solutions. To better represent real-world measurement conditions, 5% noise is added to the synthetic data, introducing realistic variability into the training process. The results demonstrate that PINNs successfully reconstruct the trajectories of $S(t)$, $I(t)$, $R(t)$, and $D(t)$with low prediction errors. The model achieves MAE values of 0.0065 (S), 0.0067 (I), 0.0208 (R), and 0.0043 (D), with corresponding RMSE values of 0.0090, 0.0074, 0.0253, and 0.0058. Moreover, the estimated parameters closely match the true values, yielding $\beta = 0.5031$, $\gamma = 0.0996$, $\delta = 0.0095$, and $\omega = 0.0149$, demonstrating strong parameter identification capability. These findings confirm that PINNs constitute a reliable and accurate framework for analyzing infectious disease dynamics and offer promising potential for extension to more complex epidemiological models and real-world datasets.

Keywords: Physics-informed neural network, SIRS-D model, Estimation parameter, Runge-kutta

Introduction

Infectious diseases remain a recurring global health challenge due to their rapid transmission and widespread impact. Many infectious diseases also exhibit the possibility of reinfection, such as seasonal influenza, pertussis, and other respiratory viral infections that do not provide long-term immunity. This phenomenon of reinfection makes epidemiological models that account for immunity loss an important component in understanding the dynamics of disease transmission (Hethcote, 2000).

The SIRS-D model itself is an extension of the SIRS model, which initially consisted of three compartments: susceptible, infected, and recovered. In the SIRS model, individuals who recover may become susceptible again after their immunity wanes, making it suitable for representing diseases that allow reinfection, including infectious diseases such as COVID-19. The SIRS-D model then adds a death compartment, allowing both reinfection dynamics and mortality risks to be represented more realistically for diseases with a certain fatality level.

- Selection and peer-review under responsibility of the Organizing Committee of the Conference

Parameter estimation in the SIRS-D model, such as the transmission rate, recovery rate, immunity loss rate, and mortality rate, plays a crucial role in understanding the characteristics of disease spread. With advancements in modern computational methods, Physics-Informed Neural Networks (PINNs) have increasingly been used because they integrate data with the mathematical structure of differential equation models, enabling the learning process to remain aligned with the true system dynamics (Raissi et al., 2019). PINNs have also been shown to be effective in various epidemiological and dynamical system studies because they can produce stable estimates even when data are limited (Cuomo et al., 2022; Millevoi et al., 2024; and Farea et al., 2025).

Several studies demonstrate that PINNs are an effective approach for analyzing dynamical systems governed by differential equations. This method has been applied in biomedicine to reconstruct cardiac electrical activation, and in epidemiology by Berkhahn & Ehrhardt (2022) and Han et al. (2024) to analyze COVID-19 transmission and estimate epidemiological parameters directly from data. In addition, Ouyoussef et al. (2024) showed that PINNs can estimate transmission parameters in a two-group epidemic model with high accuracy, while Farea et al. (2025) demonstrated that PINNs can solve forward and inverse problems in the SIR model with excellent reconstruction performance. These findings highlight the significant potential of PINNs in epidemiological model analysis, especially for parameter estimation when data availability is limited.

In this study, PINNs are used to estimate the parameters of the SIRS-D model. The training data were obtained through numerical simulation using the fourth-order Runge–Kutta method to ensure that the synthetic data generated were consistent and controlled. Through this approach, the study aims to evaluate the capability of PINNs in learning the dynamics of the SIRS-D model, assessing the quality of parameter estimation, and exploring the potential application of this method in compartmental epidemiological models for infectious diseases characterized by reinfection and notable mortality rates.

Physics-Informed Neural Networks (PINNs)

PINNs are a machine learning approach that integrates physical laws into the training process of artificial neural networks. Unlike conventional models that rely solely on observational data, PINNs incorporate differential equation systems, both ODEs and PDEs, as part of the loss function. Consequently, the resulting solution not only fits empirical data but also remains consistent with the underlying system dynamics.

In general, the architecture of PINNs consists of an input layer, several hidden layers with nonlinear activation functions, and an output layer that produces the predicted state variables $\hat{x}(t)$. Its main uniqueness lies in the combined loss function, which includes the error relative to the data and the residual of the differential equations. During training, the network seeks to minimize both components simultaneously, allowing the model to follow data patterns while still satisfying physical laws. The following is the architecture of PINNs as presented in Figure 1.

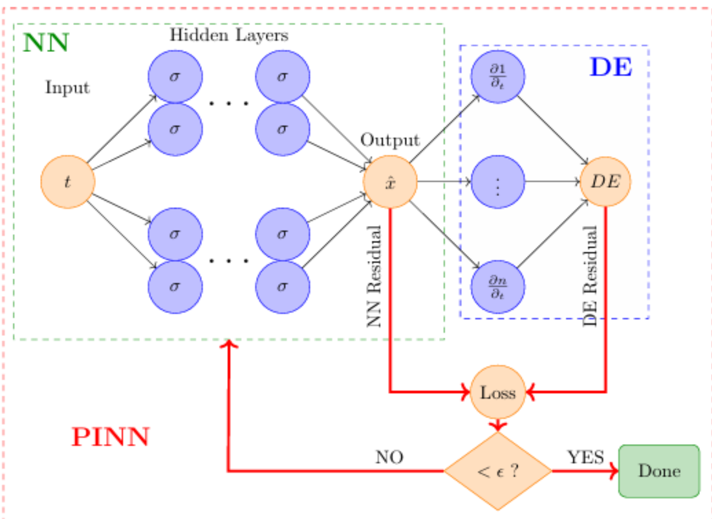

Figure 1. PINNs' architecture (Farea et al., 2025)

During training, PINNs aim to minimize the combined loss function:

$$\mathcal{L}_{total} = \lambda_1 \mathcal{L}_{data} + \lambda_2 \mathcal{L}_{physics}$$

with $\mathcal{L}_{data}$ representing the error between the neural network predictions and the observational data, while $\mathcal{L}_{physics}$ measures the extent to which the network predictions satisfy the system of differential equations. The weights λ_1 and λ_2 are used as balancing factors between accuracy with respect to the data and adherence to physical laws.

The data loss component is computed using the Mean Squared Error (MSE), whereas the physics loss evaluates the residuals of the differential system through automatic differentiation. Automatic differentiation technology, such as that provided in PyTorch, enables PINNs to compute time derivatives accurately without requiring additional numerical schemes. This approach allows PINNs to handle nonlinear problems without linearization or local time-stepping.

$$\mathcal{L}_{data} = \frac{1}{N}\sum_{i=1}^{N}(\hat{x}(t_i) - x(t_i))^2 \tag{1}$$

with $\hat{x}(t_i)$ represents the neural network's predicted value at time t_i, while $x_i$is the actual observed value at the same time.

Meanwhile, the physics loss component ensures that the solution remains consistent with the modeled dynamics:

$$\mathcal{L}_{physics} = \frac{1}{N}\sum_{i=1}^{N}\left(\frac{d\hat{x}(t_i)}{dt} - f(\hat{x}, t_i)\right)^2 \tag{2}$$

$f(\hat{x}, t_i)$ is a functional form of the system of differential equations that describes the relationships among the variables in the model and $\frac{d\hat{x}(t_i)}{dt}$ in the equation above is computed automatically using PyTorch's automatic differentiation framework.

In epidemiological modeling such as SIRS-D, PINNs can be used to estimate unknown parameters, such as the transmission rate, recovery rate, disease-induced mortality, and loss of immunity. The training process employs optimization algorithms such as Adam to update the network weights and model parameters until the loss function reaches a certain tolerance value. In this way, PINNs provide solutions that are consistent with the data while also adhering to the underlying differential system dynamics.

SIRS-D Model

The SIRS-D (Susceptible–Infected–Recovered–Susceptible–Deceased) model is an extension of compartmental epidemiological models used to analyze the dynamics of infectious disease transmission. This model originates from the basic SIR framework and is further expanded by adding a death compartment as well as a mechanism that allows recovered individuals to return to the susceptible class, thereby representing the possibility of reinfection. With this structure, the SIRS-D model provides a more realistic depiction of transmission, recovery, and disease-induced mortality.

The model divides the population into four main compartments based on their epidemiological status at time t: susceptible $S(t)$, infected $I(t)$, recovered $R(t)$, and deceased $D(t)$ (Zinihi et al., 2025). The total population $N$is assumed to remain constant over time and is defined as the sum of individuals across all compartments. In this study, the compartmental variables are expressed in proportions, such that each compartment takes values between 0 and 1, making the total population $N = 1$.

$$S(t) + I(t) + R(t) + D(t) = 1 \tag{3}$$

The dynamics of transitions between compartments are determined by four parameters. The transmission rate βdescribes the rate at which the disease spreads from infected individuals to susceptible individuals. The recovery rate γrepresents the proportion of infected individuals who recover per unit time. The parameter δcharacterizes the disease-induced mortality rate, while the parameter ωdescribes the rate of immunity loss that allows recovered individuals to become susceptible again. The presence of the parameter ωenables the SIRS-D model to capture reinfection phenomena commonly observed in certain infectious diseases. Assuming that transmission occurs through direct contact between susceptible and infected individuals, the dynamics of each compartment are expressed through the following system of differential equations:

$$
\begin{aligned}
\frac{dS(t)}{dt} &= -\beta S(t)I(t) + \omega R(t) \\
\frac{dI(t)}{dt} &= \beta S(t)I(t) - \gamma I(t) - \delta I(t) \\
\frac{dR(t)}{dt} &= \gamma I(t) - \omega R(t) \\
\frac{dD(t)}{dt} &= \delta I(t)
\end{aligned} \tag{4}
$$

Several assumptions are used to simplify the simulation process and parameter estimation using PINNs. First, the population is assumed to be closed, meaning that the total population remains constant throughout the simulation period; in other words, no births or natural deaths occur aside from disease-induced mortality. Second, transmission is assumed to occur through direct contact between susceptible and infected individuals, so the transmission rate depends on interactions between these two compartments. Third, individuals who have recovered may experience a loss of immunity and return to the susceptible class, allowing reinfection to occur. Fourth, the parameters β, γ, δ, and $\omega$are assumed to be constant over time, although their values are estimated during the PINNs training process. Fifth, the initial proportions of each compartment are assumed to be known at the start of the simulation. These assumptions are used to keep the model simple while still capturing the fundamental dynamics of disease transmission with reinfection.

Method

Data Source

This study utilizes synthetic data to evaluate the capability of Physics-Informed Neural Networks (PINNs) in estimating parameters of the SIRS-D model. The synthetic data were generated numerically based on the system of differential equations of the SIRS-D model using predetermined parameter values. The data generation process was carried out by solving the differential equation system numerically using the fourth-order Runge–Kutta (RK4) method with 5% added noise. This method was chosen due to its good accuracy and stability in modeling epidemic dynamics. Through the RK4 scheme, approximate solutions at each time step can be computed systematically, resulting in population dynamics curves for each compartment, namely $S(t)$, $I(t)$, $R(t)$, and $D(t)$.

By using fully controlled data, the performance of PINNs can be evaluated more clearly, as the true parameter values and actual underlying dynamics are known in advance. Furthermore, the use of synthetic data enables researchers to ensure that the model operates consistently before being applied to real-world data, which are typically more complex and contain observational uncertainties. The following is a plot of the data generated using the fourth-order Runge–Kutta method.

Methodology

The method used in this study is a numerical experiment based on synthetic data. The research steps are as follows:

1. Determining the basic parameters of the SIRS-D model ($\beta, \gamma, \delta, \omega$) which serve as references for generating synthetic data.
2. Generating synthetic data by constructing the SIRS-D system of differential equations and solving it using the fourth-order Runge–Kutta method to obtain the dynamics of $S(t), I(t), R(t)$,and $D(t)$.
3. Splitting the synthetic data into training and testing datasets with an 80:20 ratio (96 for training and 24 for testing).
4. Defining the architecture of the PINNs model with time $t$as input and the estimated outputs $\hat{S}(t)$, $\hat{I}(t)$, $\hat{R}(t)$,and $\widehat{D}(t)$.
5. Training the PINNs model on the training dataset by minimizing a loss function that combines prediction error on synthetic data and the residuals of the differential equations, resulting in parameter estimates consistent with the system dynamics.
6. Evaluating the PINNs model by calculating MAE and RMSE using the testing data.
7. Analyzing the parameter estimation results to assess the ability of PINNs to identify epidemiological parameters based on synthetic data.

Results and Discussion

The data used in this study consist of synthetic data generated from the SIRS-D model. The generation of synthetic data is carried out to provide a fully controlled testing environment, allowing the evaluation of the capability of Physics-Informed Neural Networks (PINNs) in estimating parameters to be performed more clearly and systematically.

This synthetic data is obtained by numerically solving the system of differential equations of the SIRS-D model using the fourth-order Runge–Kutta (RK4) method with 5% added noise. RK4 was chosen because it offers a good balance between accuracy and stability, especially when used to model the dynamics of infectious diseases. Through the RK4 scheme, approximate solutions are computed incrementally at each time step, resulting in the population evolution curves for the susceptible $S(t)$, infected $I(t)$, recovered $R(t)$, and deceased $D(t)$compartments. In this study, the data generation process was performed using predetermined baseline parameters, namely β=0.5, γ=0.1, γ=0.01, ω=0.015, $S(0)$=0.999, $I(0)$=0.001, $R(0)$=0, dan $D(0)$=0.

The simulation time span is set from $t = 0$ to $t = 60$, with a total of 120 data points, ensuring a uniform time step throughout the simulation. With this parameter configuration and numerical scheme, a series of data reflecting epidemic dynamics consistent with the SIRS-D model is obtained. These data are then used as input to train and evaluate the PINNs model. Since the true parameter values are known, the model performance can be assessed directly through the ability of PINNs to reconstruct both the parameters and the solution curves that approximate the true underlying dynamics.

Figure 1. presents the plot of the synthetic data generated using the RK4 method with 5% added noise, illustrating the population changes in each compartment over the simulation period.

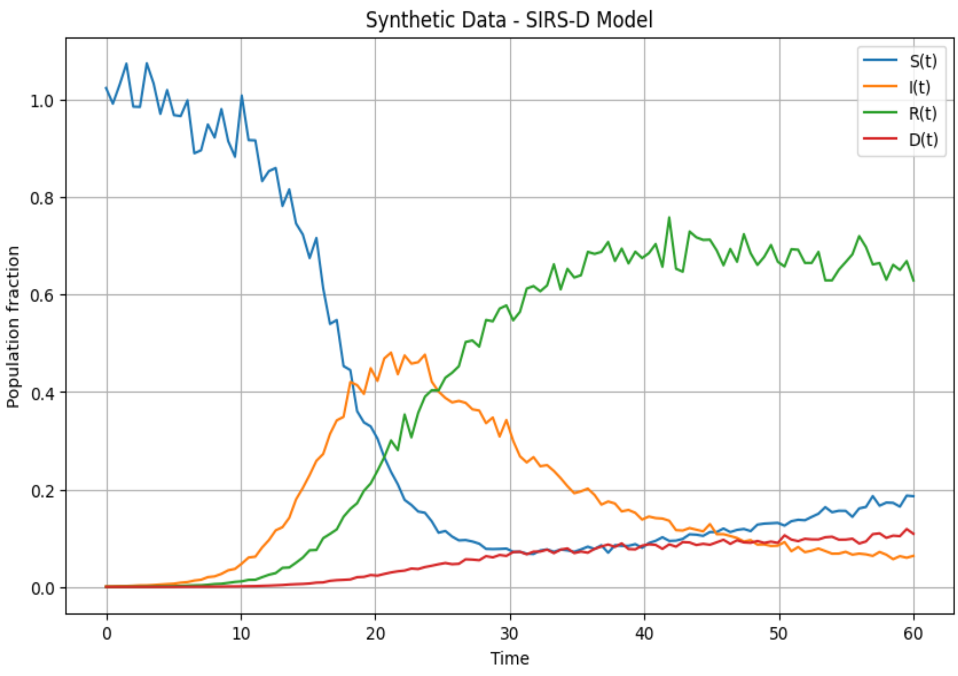

Figure 1. Synthetic data

Physics-Informed Neural Networks (PINNs) Simulation for Parameter Estimation

At this stage, the Physics-Informed Neural Networks (PINNs) model is constructed and trained to estimate the parameters and reconstruct the solution dynamics of the SIRS-D model. The entire training process is carried out using PyTorch, with the network architecture and training parameters configured to ensure stable learning from both the synthetic data and the physical information derived from the differential equations. The network architecture used is a feedforward neural network with a single input representing the time variable t, and four outputs corresponding to the functions $S(t)$, $I(t)$, $R(t)$, and $D(t)$. The network consists of three hidden layers with 30, 40, and 50 neurons, respectively. Each layer is connected through sigmoid activation functions, chosen for their smoothness and suitability in supporting automatic differentiation, which is central to the PINNs approach.

The training process is carried out using the Adam optimizer, as it is capable of accelerating convergence and performs well on complex objective functions. The learning rate is set to 1×10^{-4}, while the numerical tolerance parameter (epsilon) in the optimizer is assigned a small value of $2.9 \times 10^{-4}$to maintain computational stability during weight updates. The loss function used is a combination of data loss and physics loss, with respective weights of 0.3 and 0.7 (Farea et al., 2025). This weighting emphasizes that the network should not only fit the observational data but also satisfy the physical structure defined by the differential equations of the SIRS-D model. Through this approach, the resulting solution is expected to be mathematically consistent rather than merely following the pattern of the data points.

Training is performed for a maximum of 50,000 epochs, or terminated earlier if the model reaches convergence. Under this configuration, the total computational time required to complete the training process is approximately 2 minutes and 27 seconds, which is relatively efficient for a PINNs model with four outputs. The following presents the convergence results of the PINNs loss.

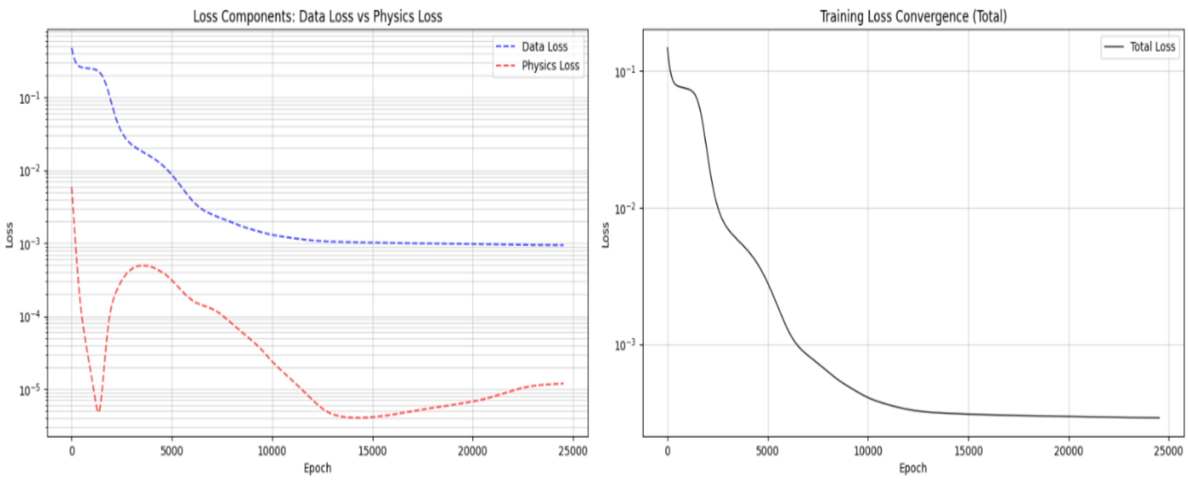

Figure 2. Convergence analysis of PINNs' loss

The left panel shows the evolution of the individual loss components during the PINNs training process, namely the data loss and the physics loss. The data loss (blue dashed curve) decreases steadily throughout training, starting from 10^{-1} and gradually approaching the order of 10^{-3}. This consistent decline indicates that the network progressively improves its fit to the synthetic observations of $S(t)$, $I(t)$, $R(t)$, and $D(t)$. In contrast, the physics loss (red dashed curve) exhibits a more dynamic pattern. At the beginning of training, its value drops sharply, followed by a temporary increase around the mid-training phase. This behavior reflects the adjustment process in PINNs, where the network simultaneously attempts to minimize the discrepancy with data and satisfy the governing differential equations. After this transitional phase, the physics loss decreases again and stabilizes at a very small magnitude, indicating that the physical constraints of the SIRS-D model are increasingly well satisfied.

The right panel presents the total training loss, which combines both data and physics components. The curve demonstrates a clear convergence pattern. In the early epochs, the total loss decreases rapidly, showing that the network quickly captures the dominant structure of the problem. As training progresses, the rate of decrease becomes more gradual, indicating parameter refinement. Toward the end of training, the total loss reaches a stable plateau at a very small value and no longer exhibits significant oscillations. This stable convergence suggests that the selected network architecture, activation function, and Adam optimizer effectively guide the training process.

Overall, both figures confirm that the PINNs model achieves a balanced optimization between data fitting and physical consistency. The stable behavior of the loss components indicates that the network has successfully learned the epidemic dynamics represented by the SIRS-D system and is ready for further evaluation through predictive analysis and visualization.

The four panels depict the evolution of the estimated parameters β, γ, δ, and ωobtained using PINNs, compared with their respective true values (red dashed lines). Each curve illustrates how the network gradually refines the parameter values throughout the training process. For β, the estimate initially starts below the true value of 0.5

and shows moderate fluctuations during the early epochs. After this initial adjustment phase, the curve increases steadily and approaches the reference value. In the later stages of training, the estimate stabilizes very close to 0.5, indicating successful convergence. A similar convergence behavior can be observed for γ. The estimated value first exhibits noticeable oscillations, including an early overshoot above the true value of 0.1, followed by a temporary decline. As training progresses, the curve gradually corrects itself and converges smoothly toward 0.1, with minimal variation near the final epochs.

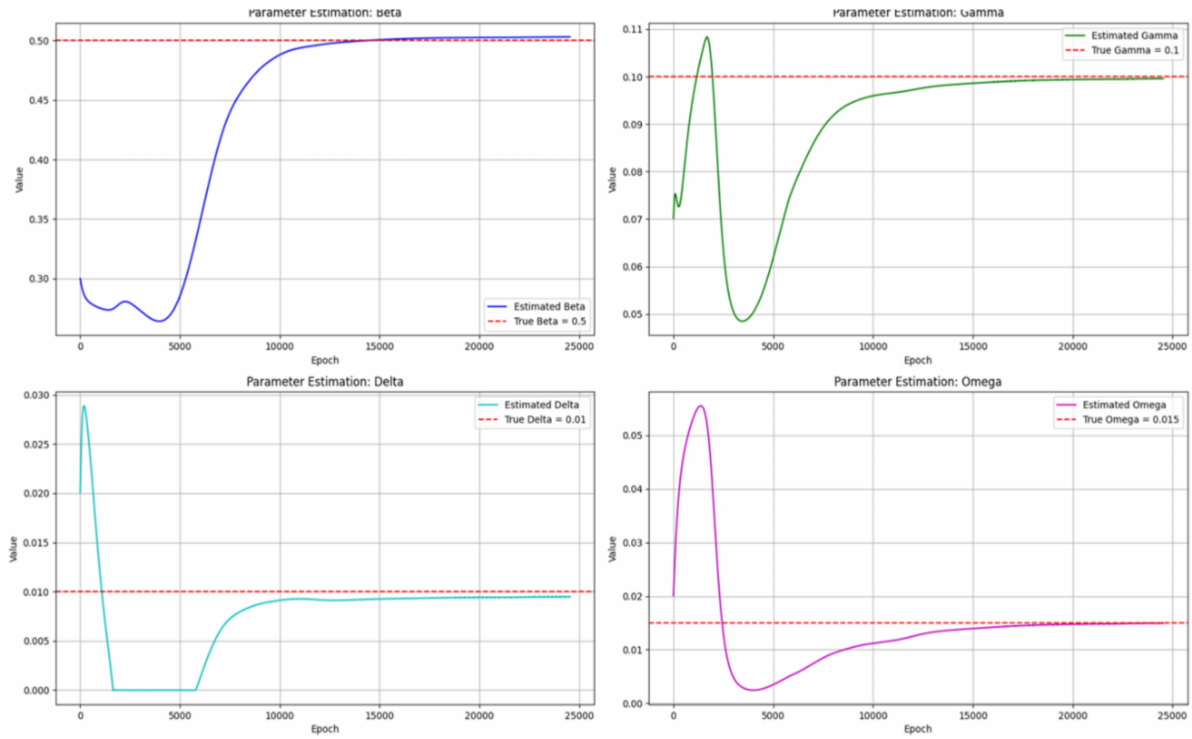

Figure 3. Convergence analysis of parameter estimation

The estimation of δshows a sharp drop at the beginning of training, reaching values close to zero. This early instability is followed by a gradual increase, and the curve eventually stabilizes near its true value of 0.01. The delayed stabilization reflects the relatively small magnitude of this parameter and its weaker influence on the system dynamics during the early learning phase. Among all parameters, ωexhibits the most pronounced early fluctuations, including a significant spike followed by a sharp decrease. However, after several thousand epochs, the estimate begins to increase steadily and ultimately converges toward the true value of 0.015. The stabilization in the final stage indicates that the network successfully captures the waning immunity effect represented by this parameter. Overall, despite the distinct transient behaviors observed in the early training phase, all parameter estimates progressively approach their true values and remain stable toward the end of training. This consistent convergence demonstrates that the PINNs framework is capable of accurately and reliably identifying the parameters of the SIRS-D model.

To evaluate the ability of the PINNs model to make predictions on the testing data, two main metrics are used: Mean Absolute Error (MAE) and Root Mean Square Error (RMSE). These metrics are commonly used to measure how closely the model's predictions match the actual values. MAE measures the average absolute difference between predictions and actual data, and is defined as:

$$MAE = \frac{1}{N}\sum_{i-1}^{N}|y_i - \hat{y}_i| \tag{5}$$

Meanwhile, RMSE provides an error measure that assigns a larger penalty to large deviations, and is expressed as:

$$RMSE = \sqrt{\frac{1}{N}\sum_{i-1}^{N}(y_i - \hat{y}_i)^2} \tag{6}$$

The following are the results of the MAE and RMSE calculations:

Table 1. Testing dataset evaluation

Variables	MAE	RMSE
S	0.0065	0.0090
I	0.0067	0.0074
R	0.0208	0.0253
D	0.0043	0.0058

Table 1 summarizes the testing performance of the PINNs model for each compartment: S, I, R, and D. The MAE and RMSE values for all variables are relatively small, lying approximately in the order of 10^{-3} to 10^{-2}. This indicates that the predicted solutions are close to the reference data across all compartments. The Scompartment yields an MAE of 0.0065 and an RMSE of 0.0090, showing good agreement between the predicted and true susceptible population. For the Icompartment, the MAE and RMSE are 0.0067 and 0.0074, respectively, which also reflect accurate reconstruction of the infected dynamics. The Rcompartment presents slightly higher errors (MAE = 0.0208 and RMSE = 0.0253) compared to the other variables. Nevertheless, these values remain relatively small and indicate that the recovery dynamics are still well captured by the model. Meanwhile, the Dcompartment exhibits the lowest error values (MAE = 0.0043 and RMSE = 0.0058), suggesting that the model effectively approximates the death dynamics despite the smaller magnitude typically associated with this compartment. Overall, the results in Table 1 demonstrate that the PINNs framework provides accurate predictions for all components of the SIRS-D system. The consistently low error values confirm that the model successfully learns the patterns contained in the synthetic dataset while preserving the underlying physical structure of the differential equations.

Following the evaluation of predictive performance, the next step is to examine the model's capability in parameter identification. This aspect is essential to verify whether the network truly captures the governing dynamics of the SIRS-D system rather than merely fitting the data. The comparison between the estimated parameters and their true values is presented in Table 2.

Table 2. True parameters vs estimation parameters

Parameters	True values	Estimation values
β	0.5	0.5031
γ	0.1	0.0996
δ	0.01	0.0095
ω	0.015	0.0149

Table 2 presents a comparison between the true parameter values of the SIRS-D model and the corresponding estimates obtained using the PINNs framework. The results demonstrate that all parameters, namely β, γ, δ, and ω, are identified with a high degree of accuracy. The estimated values are remarkably close to the true parameters, with only marginal deviations observed in the fourth decimal place. Specifically, the estimated transmission rate $\beta(0.5031)$ closely approximates its true value of 0.5. Similarly, the recovery rate $\gamma$is estimated as 0.0996, which is highly consistent with the reference value of 0.1. The mortality rate $\delta$and the waning immunity rate $\omega$are also reconstructed with minimal discrepancies, yielding estimated values of 0.0095 and 0.0149 compared to their true values of 0.01 and 0.015, respectively.

The close agreement between the true and estimated parameters confirms that the PINNs approach is capable not only of accurately reconstructing the state variables $S(t)$, $I(t)$, $R(t)$, and $D(t)$, but also of reliably identifying the intrinsic parameters governing the interactions within the SIRS-D system. This consistency indicates that the network successfully integrates observational data with the embedded physical constraints derived from the differential equations. These findings provide strong evidence that PINNs constitute an effective framework for parameter identification in epidemiological models, particularly when the training process is supported by well-defined physical structures and high-quality data. Following the parameter estimation analysis and the evaluation of predictive accuracy using MAE and RMSE metrics, the next step is to visually compare the PINNs predictions with the synthetic data over both the training and testing intervals. The subsequent figure illustrates the model's capability in reconstructing the overall epidemic dynamics represented by $S(t)$, $I(t)$, $R(t)$, and $D(t)$.

The graph below illustrates the comparison between the synthetic data and the PINNs predictions for $S(t)$, $I(t)$, $R(t)$, and $D(t)$over both the training and testing intervals. The vertical dashed line indicates the boundary between the training and testing regions. Within the training domain, the predicted trajectories closely follow the observed data points for all compartments. The susceptible population $S(t)$exhibits a gradual decline, which is accurately captured by the model. The infected compartment $I(t)$shows a clear epidemic peak followed by a steady decrease, and this characteristic pattern is well reconstructed by the PINNs solution. Similarly, the recovered population

$R(t)$demonstrates a monotonic increase before approaching saturation, while the deceased compartment $D(t)$grows progressively over time. These dynamic behaviors are consistently reproduced by the predicted curves, indicating that the network successfully learns the intrinsic structure of the epidemic process.

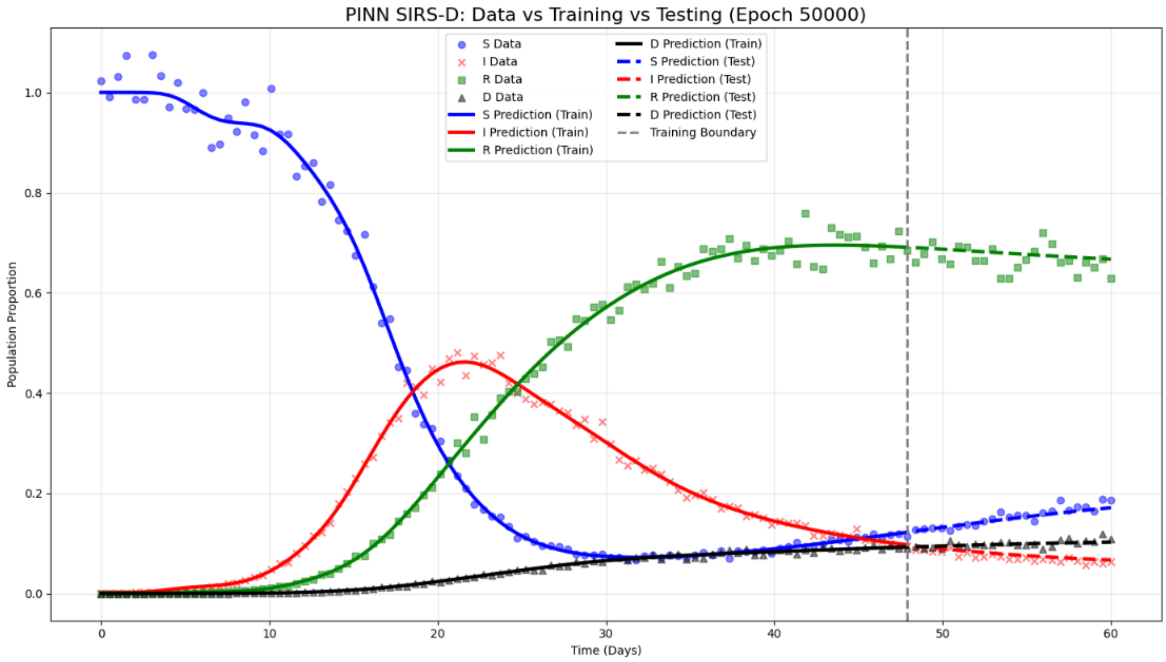

Figure 4. Comparison of real data and PINN predictions for the SIRS-D model

Importantly, the agreement between predictions and data remains strong in the testing region beyond the training boundary. The smooth continuation of all trajectories without significant deviation suggests that the model does not merely interpolate within the training data but is also capable of generalizing the learned dynamics to unseen time intervals. Overall, the close alignment between synthetic data and predicted solutions across all compartments confirms the robustness and reliability of the PINNs framework in representing the SIRS-D epidemic dynamics. The results demonstrate that the model effectively integrates observational information with the governing differential equations to produce accurate and physically consistent predictions.

Conclusion

This study demonstrates that Physics-Informed Neural Networks (PINNs) are capable of accurately reconstructing the dynamics of the SIRS-D model and estimating epidemiological parameters using synthetic data generated through the fourth-order Runge–Kutta (RK4) method with 5% added noise. The use of RK4 enables the production of smooth, stable, and system-consistent data, providing a strong foundation for evaluating the capability of PINNs.

The training process yields stable loss convergence, as reflected by the decreasing data loss and physics loss to very small values. Evaluation using MAE and RMSE metrics shows that the PINNs predictions closely match the testing data across all compartments, $S(t)$, $I(t)$, $R(t)$, dan $D(t)$, indicating highly accurate reconstruction of the solution trajectories. The parameter identification results also demonstrate strong performance, with the estimated values of β, γ, δ, and ωbeing nearly identical to the true parameters used in generating the synthetic data. This high level of agreement confirms that PINNs not only fit the data well but also effectively capture the physical structure of the differential equations underlying the SIRS-D model.

Overall, this study shows that PINNs are an effective and reliable approach for learning the dynamics of differential equation–based disease models, both in predicting solution trajectories and estimating fundamental model parameters. These findings open opportunities for further applications to other epidemiological models, including those involving real-world data that are more complex and contain substantial uncertainty.

Recommendations

This study uses synthetic data to ensure that PINNs are capable of reconstructing the SIRS-D dynamics and estimating parameters under idealized conditions. For future work, it is recommended to apply the model to real-world data (e.g., daily case reports from health agencies or publicly available epidemiological datasets) so that the performance of PINNs can be evaluated under more realistic and uncertainty-prone conditions. When transitioning to real data, several considerations should be taken into account: perform data cleaning and preprocessing (handling missing values, applying smoothing if necessary, and normalization), adjust the loss formulation to address noise (e.g., by adding regularization or using robust loss functions), and consider time-varying parameters to capture actual changes in epidemiological dynamics.

Scientific Ethics Declaration

* The scientific ethical and legal responsibility of this article published in EPSTEM Journal belongs to the authors.

Conflict of Interest

* The authors have no conflicts of interest in any area.

Funding

* The author would like to express sincere gratitude to the Indonesia Endowment Fund for Education (LPDP) under the Ministry of Finance of the Republic of Indonesia for supporting and funding this research. Their support has been instrumental in facilitating the completion of this work.

Acknowledgements or Notes

* This article was presented as an oral presentation at the International Conference on Basic Sciences and Technology (www.icbast.net) held in Konya/Türkiye on April 02-05, 2026.

* The author would like to express sincere gratitude to the Indonesia Endowment Fund for Education (LPDP) under the Ministry of Finance of the Republic of Indonesia for providing financial support for this research. The author also appreciates the guidance and insightful discussions from the academic supervisor, as well as the encouragement and support from colleagues and family throughout this study.

References

Berkhahn, S., & Ehrhardt, M. (2022). A physics-informed neural network to model COVID-19 infection and hospitalization scenarios. *Advances in Continuous and Discrete Models, 2022*(1), 61.

Cuomo, S., Schiano Di Cola, V., Giampaolo, F., Rozza, G., Raissi, M., & Piccialli, F. (2022). Scientific machine learning through physics-informed neural networks: Where we are and what's next. *Journal of Scientific Computing, 92*(3), 88.

Farea, A., Yli-Harja, O., & Emmert-Streib, F. (2025). Using physics-informed neural networks for modeling biological and epidemiological dynamical systems. *Mathematics, 13*(10), 1664.

Han, S., Stelz, L., Stoecker, H., Wang, L., & Zhou, K. (2024). Approaching epidemiological dynamics of COVID-19 with physics-informed neural networks. *Journal of the Franklin Institute, 361*(6), 106671.

Hethcote, H. W. (2000). The mathematics of infectious diseases. *SIAM Review, 42*(4), 599–653.

Millevoi, C., Pasetto, D., & Ferronato, M. (2024). A physics-informed neural network approach for compartmental epidemiological models. *PLOS Computational Biology, 20*(9), e1012387.

Ouyoussef, K. I., El Karkri, J., Tine, L. M., & Aboulaich, R. (2024). Physics-informed neural networks for parameter estimation and simulation of a two-group epidemiological model. *International Journal of Modeling, Simulation, and Scientific Computing, 15*(3), 2450042.

Raissi, M., Perdikaris, P., & Karniadakis, G. E. (2019). Physics-informed neural networks: A deep learning framework for solving forward and inverse problems involving nonlinear partial differential equations. *Journal of Computational Physics, 378*, 686–707.

Zinihi, A., Ehrhardt, M., & Sidi Ammi, M. R. (2026). A Koopman operator framework for nonlinear epidemic dynamics: Application to an SIRSD model. *Nonlinear Science, 6*, 100095.

Author(s) Information

Fitri Cahyani
Universitas Gadjah Mada
Yogyakarta, Indonesia
ORCID iD: https://orcid.org/0009-0006-8290-6763
*Contact e-mail: *fitricahyani192@gmail.com*

Abdurakhman Abdurakhman
Universitas Gadjah Mada
Yogyakarta, Indonesia
ORCID iD: https://orcid.org/0000-0003-0758-5323

Chyntia Meininda Anjanni
Universitas Gadjah Mada
Yogyakarta, Indonesia
ORCID iD: https://orcid.org/0009-0002-5108-6759

*Corresponding author(s) email

To cite this article:

Cahyani, F., Abdurakhman, A. & Anjanni, C. M., (2026). Physics-informed neural networks (PINNs) for parameter estimation in the SIRS-D epidemiological model. *The Eurasia Proceedings of Science, Technology, Engineering and Mathematics (EPSTEM), 40,* 526-536.